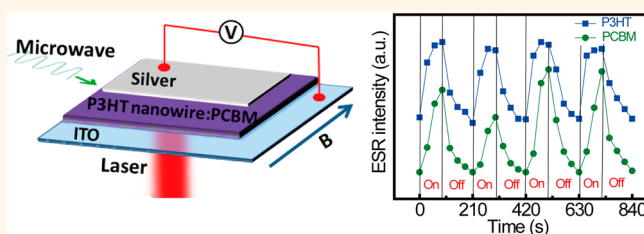# Charge-Transfer Magnetoelectrics of Polymeric Multiferroics

Wei Qin,[†] Daniel Jasion,[†] Xiaomin Chen,[‡] Manfred Wuttig,[‡] and Shenqiang Ren[†,*]

[†]Department of Chemistry, University of Kansas, Lawrence, Kansas 66045, United States and [‡]Department of Materials Science and Engineering, University of Maryland, College Park, Maryland 20742, United States

ABSTRACT The renaissance of multiferroics has yielded a deeper understanding of magneto-electric coupling of inorganic single-phase multiferroics and composites. Here, we report charge-transfer polymeric multiferroics, which exhibit external field-controlled magnetic, ferroelectric, and microwave response, as well as magneto-to-dielectric coupling. The charge-transfer-controlled ferroic properties result from the magnetic field-tunable triplet exciton which has been validated by the dynamic polaron−bipolaron transition model. In addition, the temperature-dependent dielectric discontinuity and electric-field-dependent polarization confirms room temperature ferroelectricity of crystalline charge-transfer polymeric multiferroics due to the triplet exciton, which allows the tunability of polarization by the photoexcitation.

KEYWORDS: organic multiferroics · charge transfer · ferroelectricity · magneto-electric coupling

Magneto-electric (ME) coupling of multiferroics or metamaterials, showing dual electrical and magnetic degrees of freedom, has drawn increasing interest because of their tailored magnetic permeability and dielectric permittivity for potential applications, such as multiple-state memories,[1] ultrasensitive magnetic field sensors,[2] and ME data storage and switching.[3,4] The majority of inorganic single-phase multiferroics have classically been of the perovskite structure, such as $YMnO_3$,[5] $TbMnO_3$,[6,7] and $BiFeO_3$.[8−10] In these materials, magnetic order originates from the unpaired spin of Mn or Fe ions. In addition to these inorganic multiferroics, organic charge-transfer materials offer promising new routes toward room temperature multiferroics.[11−14] Polymer charge-transfer composites based on poly(vinylidene fluoride-co-trifluoroethylene) and the single-crystalline salt κ-(BEDT-TTF)$_2$CuTN(CN)$_2$UCl have shown magnetic and multiferroic properties.[15,16] In 2011, we reported room temperature excitonic magnetism of one-dimensional organic charge-transfer heterojunction caused by the overlap between the spin density and charge density waves, in which the crystalline-induced dipole ordering could potentially yield ferroelectricity.[14] Supramolecular charge-transfer complexes

indeed have shown room temperature ferroelectricity due to the donor−acceptor dimerization and a polar lattice.[17] Furthermore, density functional theory calculations have predicted the crystallized transition-metal benzene,[18] fused azulene system,[19] [(CH$_3$)$_2$NH$_2$]Co(HCOO)$_3$,[20] and [(CH$_3$)$_2$NH$_2$]-Cr(HCOO)$_3$[21] as potential multiferroics with high ME coupling coefficient. Although the unique ferroic coupling mechanism of organic charge-transfer materials lags behind its inorganic counterparts, organic multiferroics is attracting considerable attention for their potential applications, such as magnetic field effect on organic optoelectronics,[22,23] molecular spintronics,[24] charge-transfer-based sensitizers for photovoltaics,[17] and tunable microwave ME devices.[12]

Here, we report external field-controlled magnetic, ferroelectric, magneto-dielectric, and microwave characteristics of charge-transfer polymeric multiferroics. The ME coupling mechanism is further validated through use of the dynamic polaron−bipolaron transition model. In addition, we demonstrate (1) temperature-dependent magnetic susceptibility in crystalline polymeric multiferroics by tuning the fullerene acceptor ratio, (2) spin-correlated transport behavior of crystalline polymeric multiferroics due to the polaron and bipolaron
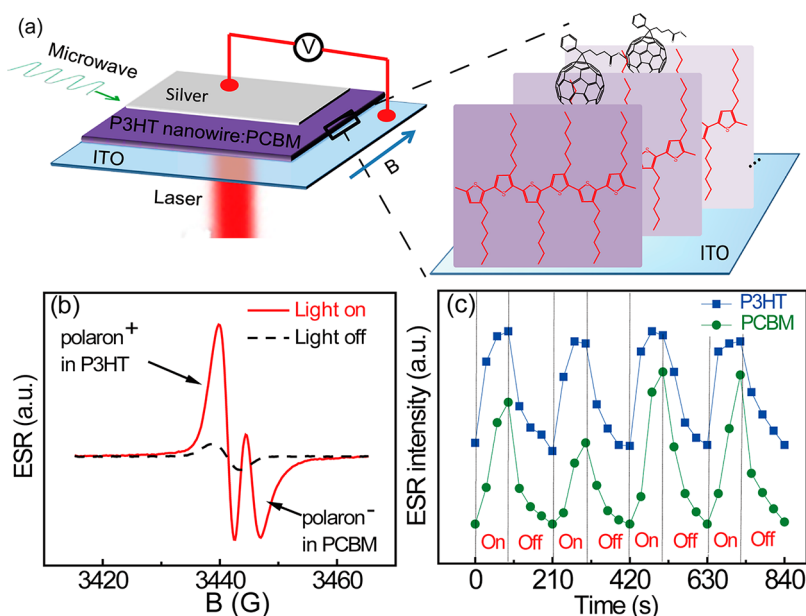
Figure 1. Schematic diagram of device and ESR of P3HT:PCBM complex. (a) Schematic diagram of ITO/P3HT:PCBM/Ag device. (b) ESR of P3HT:PCBM composite with and without light. (c) ESR intensity response with light on/off cycles.

ratio-dependent resistance, (3) electric-field-tuned susceptibility (increasing by 14%) and magneto-dielectric coupling through the control of the ratio between singlet and triplet charge transfer states, and (4) room temperature ferroelectricity and its tunability through the exciton density.

RESULTS AND DISCUSSION

By applying a magnetic field and microwave radiation, the transition between spin-up and spin-down electrons can take place in polymeric multiferroic materials (Figure 1a), in which the microwave frequency, v, obeys the relation: $hv = g\mu_B B$, where h represents Planck's constant, μ_B the Bohr magneton, and B the external magnetic field. Figure 1b presents the light-induced electron spin resonance (ESR) spectra of poly(3-hexylthiophene) nanowires (nw-P3HT) and 1-(3-methoxycarbonyl)propyl-1-phenyl[6,6]C61 (PCBM) multiferroics. The surface morphology of nw-P3HT:PCBM polymeric multiferroics and the detailed ESR spectra at different ratios and temperatures are shown in the Figures S1 and S2 of Supporting Information. In organic materials, the delocalized excited charge carriers (electrons or holes) are trapped by molecular deformation, creating polarons (spin $\pm 1/2$). As shown in Figure 1b, the ESR peaks (solid line) are caused by the positive polaron of the nw-P3HT and negative polarons on the PCBM phase, which are excited by charge-transfer states. The slight shift of the resonance peaks is caused by the different g factors. It should be noted that the spin resonance can be reversibly tuned by shining the light on or off cycles (Figure 1c). By applying photoexcitation, the ESR intensity increases drastically in both P3HT nanowire and PCBM phase. The ESR signal starts to decay when the light is off.

The composition of polymeric multiferroics significantly influences their magnetic characteristics. As the carrier density increases, induced by photoexcitation and charge-transfer separation, the overlap of two neighboring polarons will be enhanced, which leads to a higher probability of forming bipolarons. An equal ratio of polymeric multiferroics ((nw-P3HT)$_{0.5}$(PCBM)$_{0.5}$) has been widely exploited in organic bulk hetero-junction optoelectronics, in which a large interfacial area could significantly enhance the carrier density from charge-transfer states,[25,26] leading to the bipolaron becoming the majority carrier. In comparison, the bipolaron acts as the minority carrier in (nw-P3HT)$_{0.25}$(PCBM)$_{0.75}$ and (nw-P3HT)$_{0.75}$(PCBM)$_{0.25}$ because of relatively small excited carrier density from charge transfer. For a given material, if the ESR line width is fixed, the presence of a strong ESR signal (the detailed ESR spectra measurement is in Supporting Information) indicates a large magnetic susceptibility. Therefore, the high singlet bipolaron ratio in the (nw-P3HT)$_{0.5}$(PCBM)$_{0.5}$ lends itself to a low susceptibility at low temperatures, as shown in Figure 2a (solid line). The susceptibility of (nw-P3HT)$_{0.5}$(PCBM)$_{0.5}$ reaches the maximum at 150 K and then decreases with temperature, which can be attributed to the thermal excitation of the singlet bipolarons (no spin) to triplet bipolarons (with spin). In addition, the thermally excited triplet bipolarons could enhance the magnetization of (nw-P3HT)$_{0.5}$(PCBM)$_{0.5}$ polymeric multiferroics (the temperature-dependent magnetization details are shown in Figure S2 of Supporting Information). At low temperatures, the ratio of triplet bipolarons is small; however, by increasing the temperature, the singlet bipolarons can be converted to the triplet ones.[27,28] The difference in the
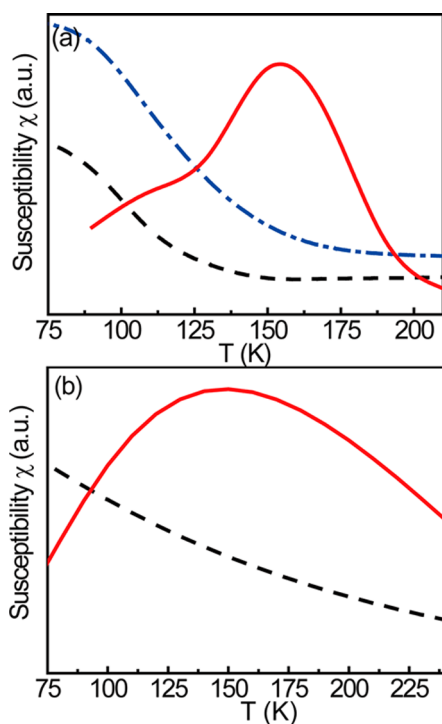
Figure 2. Temperature-dependent susceptibilities of nw-P3HT:PCBM complex. (a) Temperature tunability of the susceptibilities in systems (nw-P3HT)$_{0.25}$(PCBM)$_{0.75}$ (dashed line), (nw-P3HT)$_{0.5}$(PCBM)$_{0.5}$ (solid line), and (nw-P3HT)$_{0.75}$(PCBM)$_{0.25}$ (dash-dotted line). (b) Theoretical calculations of the temperature-dependent susceptibilities on the systems (nw-P3HT)$_{0.25}$(PCBM)$_{0.75}$ and (nw-P3HT)$_{0.75}$(PCBM)$_{0.25}$ with minority (dashed line) and majority (solid line) bipolaron in (nw-P3HT)$_{0.5}$(PCBM)$_{0.5}$.

probability distribution between spin-up and spin-down also decreases with increasing temperature, leading to a decrease of magnetic susceptibility above 150 K.

To further understand the temperature-dependent susceptibility behavior, we present a theoretical model to reveal the relationship between the spin and bipolaron. We designate the excited carriers to be singlet polaron pairs, triplet polaron pairs, singlet bipolarons, and triplet bipolarons. When a magnetic field is applied or temperature is changed, transitions among them will take place. Introducing the transition rate γ_T to describe the conversion from a triplet polaron pair to a singlet one and γ_S for its reverse process, we write the dynamic transition equations of these carriers as

$$
\begin{aligned}
\frac{dn_{pp\text{-}S}}{dt} &= +\gamma_T n_{pp\text{-}T} - \gamma_S n_{pp\text{-}S} + k n_{bp\text{-}S} - b n_{pp\text{-}S} \\
\frac{dn_{pp\text{-}T}}{dt} &= -\gamma_T n_{pp\text{-}T} + \gamma_S n_{pp\text{-}S} + k' n_{bp\text{-}T} - b' n_{pp\text{-}T} \\
\frac{dn_{bp\text{-}S}}{dt} &= -k n_{bp\text{-}S} + b n_{pp\text{-}S} - c(T) n_{bp\text{-}S} \\
\frac{dn_{bp\text{-}T}}{dt} &= -k' n_{bp\text{-}T} + b' n_{pp\text{-}T} + c(T) n_{bp\text{-}S}
\end{aligned}
\tag{1}
$$

where $n_{pp\text{-}S}(n_{pp\text{-}T})$ is the singlet (triplet) polaron pair density and $n_p = 2(n_{pp\text{-}S} + n_{pp\text{-}T})$, and $n_{bp\text{-}S}(n_{bp\text{-}T})$ is the

density of the singlet (triplet) bipolaron. The parameter b (b') describes the local recombination rate for two polarons forming a singlet (triplet) bipolaron, while k (k') describes the reverse process, where a singlet (triplet) bipolaron decomposes into two polarons. The $c(T)$ represents the transition from singlet bipolaron to triplet bipolaron triggered by thermal excitation. The $n_p/n_{bp\text{-}T} = \xi T^2$ can be resolved from ref 28. Combining this with eq 1, we can rewrite the transition coefficient $c(T)$ (details are shown in the Supporting Information) as

$$
c(T) = k \frac{\xi T^2 (\gamma_{ap} + \gamma_{ap}') - \dfrac{b'}{k'}\gamma_{ap}'}{-b\xi T^2 - \xi T^2(\gamma_{ap} + \gamma_{ap}') + b\dfrac{b'}{k'} + \gamma_{ap}'\dfrac{b'}{k'} + \dfrac{b}{k'}\gamma_{ap}}
\tag{2}
$$

Normally in an organic semiconductor, a polaron (or bipolaron) is tightly confined at one or a few molecules as a consequence of the strong electron−lattice interactions. In this case, the interaction between the localized polaron spin, $\hat{\vec{S}}$, and the hydrogen nuclei spins, $\hat{\vec{I}}$, become apparent. If the effects of Zeeman interaction and exchange interaction of the polaron pair are considered, the total Hamiltonian for the polaron pair can be written as

$$
\hat{H} = \sum_{i=1}^{2}(g\mu_B B\hat{S}_{z,i} + a\hat{\vec{I}}_i \cdot \hat{\vec{S}}_i) + J\hat{\vec{S}}_1 \cdot \hat{\vec{S}}_2
\tag{3}
$$

where g is the Lande factor, a is the strength of the hyperfine interaction, and J denotes the exchange interaction of the polaron pair. According to the methods in our previous work,[29] we can denote the transition rate from triplet polaron pairs to singlet ones as

$$
\gamma_T = \frac{1}{16}\Bigg[4 - \frac{(\omega^2 + \frac{1}{2}J^2 + \omega J)^2}{4(a^2 + \omega^2 + \frac{1}{2}J^2 + \omega J)^2} - \frac{(\omega^2 + \frac{1}{2}J^2 - \omega J)^2}{4(a^2 + \omega^2 + \frac{1}{2}J^2 + \omega J)^2}\Bigg]\gamma_0
$$

and the rate from singlet polaron pairs to triplet ones as

$$
\gamma_S = \frac{1}{16}\Bigg[12 + \frac{(\omega^2 + \frac{1}{2}J^2 + \omega J)^2}{4(a^2 + \omega^2 + \frac{1}{2}J^2 + \omega J)^2} + \frac{(\omega^2 + \frac{1}{2}J^2 + \omega J)^2}{4(a^2 + \omega^2 + \frac{1}{2}J^2 + \omega J)^2}\Bigg]\gamma_0
$$

where $\omega = g\mu_B B$ is a parameter which is related to external magnetic field and γ_0 is a parameter.

In most materials, the susceptibility follows a Curie' law: $\chi_p \propto (n_p/T)\mu_B^2$. Therefore, temperature can induce a decrease of susceptibility. However, when the effect

of triplet bipolaron is taken into account, the total susceptibility can be expressed as

$$\chi = \chi_p + \chi_{bp-T} \propto \frac{n_p}{T}\mu_B^2 + \frac{n_{bp-T}}{T}(2\mu_B)^2 \qquad (4)$$

By solving eq 1, the susceptibility when the bipolaron is either majority (solid line) or minority (dashed line) was calculated, as shown in Figure 2b. If the singlet bipolaron comprises the majority at low temperature, the susceptibility increases first and then decreases with temperature. As the temperature increases, the singlet bipolarons could transfer into the triplet states to enhance the susceptibility. It should be noted that the susceptibility decreases as the temperature increases based on Curie's law. Therefore, temperature-dependent susceptibility is determined by the competition between thermally excited triplet bipolaron from singlet ones and Curie's law. Our calculations demonstrate that thermally excited triplet bipolarons dominate the susceptibility at temperatures below 150 K and then by Curie's law at temperatures above 150 K. Therefore, in the system where bipolarons form the majority, susceptibility first increases and then decreases with temperature. However, if the singlet bipolarons are in the minority, few triplet bipolarons are transferred from singlet states, which causes Curie's law to dominate the temperature-dependent susceptibility. Therefore, in this case, the susceptibility decreases with temperature (see the dashed line of Figure 2b).

Temperature-dependent susceptibility is due to the ratio tunability between polaron and bipolaron. Considering the different mobility of bipolaron and polaron, temperature could also tune the polaron- and bipolaron-controlled conductance. The temperature-dependent transport properties of polymeric multiferroic thin films were measured under the composition of $(nw\text{-}P3HT)_{0.5}(PCBM)_{0.5}$ (the following characterizations are based on such composition, if no other indications), as shown in the solid line of Figure 3. The resistance of the polymeric multiferroics is significantly increased as the temperature increases to 150 K
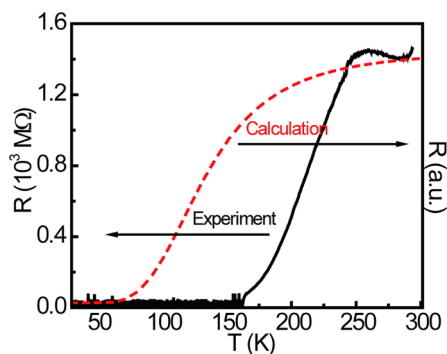
Figure 3. Temperature-dependent resistance. Resistance is measured from low temperature to room temperature (solid line); dashed line is the theoretical calculation.

(Figure 2). It should be noted that the resistance is determined by the densities of the polaron, singlet bipolaron, and triplet bipolaron and their mobilities. In general, the mobility of a polaron is greater than that of the bipolaron. This resistance can be written as $R \propto 1/(\mu_p n_p + \mu_{bp} n_{bp-T} + \mu_{bp} n_{bp-S})$. The calculated result is shown for $\mu_p = 2\mu_{bp}$ in Figure 3. At low temperatures, the ratio between polaron and bipolaron can be slightly tuned by temperature, leading to a small variation of the resistance. At temperatures above 150 K, where a large number of triplets is thermally excited, the resistance increases. Thermally activated charge hopping transport in organic materials, where charge carriers migrate from one site to the next, is not taken into account in our model. This omission leads to the slight difference between the calculated critical temperature and the measured value.

The ME coupling effect (the induction of magnetization by an electric field or of electric polarization by a magnetic field) could yield entirely new multifunctional organic material paradigms. A significant change of electron spin resonance is observed (Figure 4a) under external electric field. It is noted that, by increasing external electric field, the susceptibility increases, and it shows the reversible and repeatable electric-field-dependent susceptibility at room temperature (the details are shown in Figure S5 of the Supporting Information). In terms of the magneto-dielectric coupling, the dielectric constant increases under an applied magnetic field (Figure 4b). It should be noted that the charge-transfer polymeric multiferroics exhibit magneto-elastic effect,[14] and a relatively small elastic constant of polymer generates the resonant frequency in the MHz range. More importantly, the magneto-dielectric coupling of polymeric multiferroics could enable the tunability of the resonance frequency (from 3.8 to 5.5 MHz, Figure 4b) under a bias magnetic field of 120 mT. The dielectric change can be attributed to the magnetic-field-tunable electric polarization. It is known that the exciton has a dipole, and the polarization is associated with a large density of excitons. In organic materials, the lifetime of singlet excitons ranges from picoseconds to nanoseconds, but triplet excitons can survive over time scales of microseconds or longer.[30,31] Compared to singlet excitons, the lifetimes of the triplet excitons are extremely long. Thus only triplet excitons can contribute to the polarization. In our previous work,[32] we have shown the magnetic-field-dependent singlet and triplet charge-transfer states in organic materials, in which the triplet state ratio increased with external magnetic field. These calculations were performed taking into account the Zeeman interaction, the hyperfine interaction, and the electron−hole pair's exchange interaction. Considering that charge-transfer states act as transition states, they could dissociate into free negative and positive polarons or form excitons. Therefore, an applied
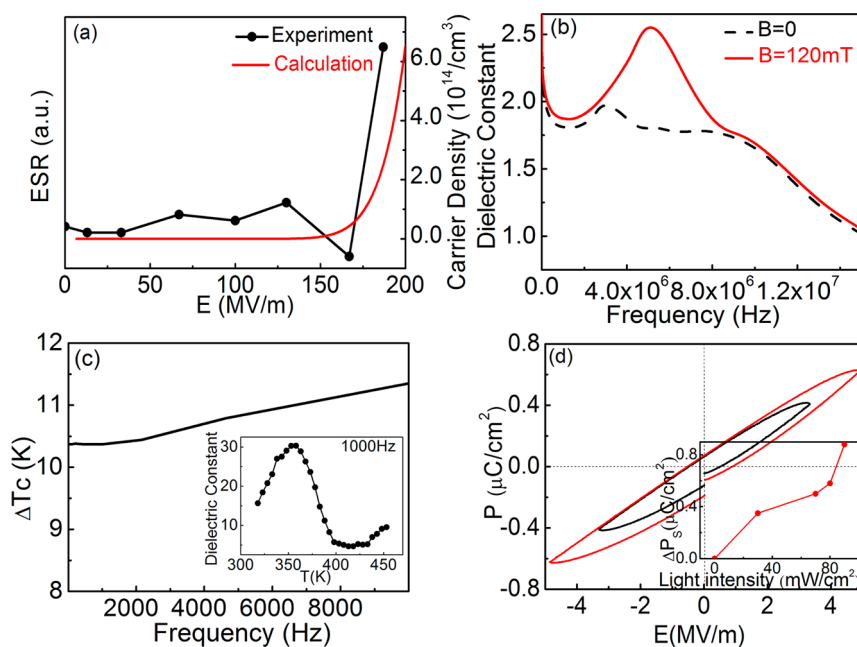
Figure 4. ME coupling and ferroelectricity. (a) Electric field tunes ESR at room temperature. (b) Magneto-dielectric coupling of polymeric multiferroics. (c) Frequency-dependent change of transition temperature; the inset shows temperature-dependent dielectric constant. (d) Polarization hysteresis loop; the inset shows polarization saturation value increase with increasing light intensity.

external magnetic field could increase the ratio of triplet excitons to increase the polarization. As different from traditional magneto-dielectric materials, such as superparamagnetic Fe_3O_4-doped polymers, the organic crystalline multiferroics could enable magneto-dielectric coupling in low density soft materials, which opens up its potential applications in electromagnetic shielding/absorbent systems around MHz.

To further verify the presence of magneto-dielectric coupling, an external magnetic field was applied to examine its effect on the frequency-dependent transition temperature $\Delta T_C = T_C(B = 0) - T_C(B)$, as shown in Figure 4c. It is found that the external magnetic field could effectively tune the transition temperature ($\Delta T_C \approx 10.5$ K is observed, which is weakly dependent on the frequency). Upon increasing the magnetic field, the transition temperature slightly decreases, shifting toward room temperature. As mentioned above, the magnetic field can induce the increase of triplet exciton, and because of the smaller radius of the triplet exciton,[33] the exchange interaction will increase with magnetic field. The transition temperature is determined by exciton exchange interaction $T_C \propto T_0 + (\alpha/(J^2 - \beta^2))$[34] (details are shown in the Supporting Information), where α and β are material-dependent parameters. Therefore, the transition temperature decreases as a magnetic field is applied to polymeric multiferroic devices. The inset of Figure 4c presents the temperature-dependent dielectric constant. The dielectric discontinuity observed at 350 K (transition temperature) suggests room temperature ferroelectricity. Further evidence for room temperature

ferroelectricity (as shown in Figure 4d) is obtained by measuring the hysteresis loop of electric-field-dependent polarization in the crystalline polymeric multiferroics. To further confirm the ferroelectricity of the polymeric sample, the positive-up/negative-down (PUND) measurement is used to evaluate the switchable ferroelectric polarization. Polarization produced by the nonswitching pulses does not go to zero, and the value is 0.05 $\mu C/cm^2$ (as shown in Supporting Information). If it is a nonferroelectric material, the value will go back to zero. The PUND response further confirms a weak ferroelectric behavior in the nw-P3HT: PCBM polymeric multiferroic system. With the effect of external electric field, the ordering of dipoles from triplet excitons induces the polarization. Under photoexcitation, more excitons are introduced to enhance the saturation polarization (P_S) with the light-intensity-dependent behavior, as shown in the inset of Figure 4c (details are shown in Supporting Information). As presented in our previous work,[14] illumination significantly enhances triplet exciton excitation in charge-transfer nw-P3HT and fullerene complex, which contributes to the excitonic magnetism. Therefore, photons can effectively improve the ferromagnetism and ferroelectricity in an organic charge-transfer crystalline complex through tuning triplet exciton density.

CONCLUSIONS

The ME coupling of charge-transfer polymeric multiferroics is demonstrated in the photoactive thiophene nanowire donor and the fullerene acceptor complex.

By tuning the ratios between the donor and acceptor, the susceptibilities present different tendency with temperature, which results from the formation of thermally excited triplet bipolarons from singlet ones. The magneto-dielectric coupling present in the polymeric multiferroics further confirms that an external magnetic field could enhance the formation of triplet excitons through tuning the ratio between singlet and triplet charge-transfer states, leading to an increased polarization. Therefore, the induced room temperature ferroelectricity shows a large tunability under the photoexcitation. Furthermore, the theoretical model established in this study provides the physical explanations for the ME coupling of polymeric multiferroics, and the dielectric discontinuity indicates the ferroelectricity of organic charge-transfer multiferroics. This discovery can provide a platform to explore multifunctional organic material applications, such as magnetic field sensors, organic microwave nanoelectronics, and organic magnetic random-access memories.

EXPERIMENTAL SECTION

Synthesis of P3HT Nanowire. First, P3HT was dissolved by 1,2-dichlorobenzene (1,2-DCB) (20 mg/mL) in a glovebox. Then acetonitrile (ACN) was added into the P3HT solution (usually adding 5−10% ACN into P3HT solution) at room temperature followed by low power ultrasonic agitation (3−5 min). At last, when solution was placed into the glovebox overnight at room temperature, the solution color changed to dark brown after the P3HT nanowires were formed.

Device Structure. ITO was chosen as the bottom electrode. After the ITO substrate was cleaned, PEDOT was coated on it at 3500 rpm for 1 min. The active layer was the nw-P3HT:PCBM composite with a concentration of 10 mg/mL in 1,2-DCB, which wa applied using a spin-coater at 1000 rpm for 1 min, which produces a thin layer that is about 150 nm thick. Silver is chosen as the top electrode through thermal evaporation. The device area is about 3×10 mm^2.

ESR Measurement. (i) Electric-field-dependent ESR at room temperature: Applied magnetic field was parallel to the surface of the device. The microwave frequency used was 9.63 GHz, and the ESR measurements were the average of 10 sweeps. The light beam path was perpendicular to the device surface through the ITO side. (ii) Low temperature ESR: First the nw-P3HT and PCBM solution was mixed together, and then the mixed solution was stirred about 8 h at room temperature. After being stirred, 150 μL of solution was taken out and injected into a glass tube. Then a light beam was added on the bottom of the glass tube for ESR measurement. A laser with a wavelength of 635 nm was used as the light beam.

Conflict of Interest: The authors declare no competing financial interest.

Supporting Information Available: Description of ESR measurements and calculation details. This material is available free of charge *via* the Internet at http://pubs.acs.org.

REFERENCES AND NOTES

1. Zavaliche, F.; Zhao, T.; Zheng, H.; Straub, F.; Cruz, M. P.; Yang, P. L.; Hao, J.; Ramesh, R. Electrically Assisted Magnetic Recording in Multiferroic Nanostructures. *Nano Lett.* **2007**, *7*, 1586–1590.
2. Greve, H.; Woltermann, E.; Quenzer, H. J.; Wagner, B.; Quandt, E. Giant Magnetoelectric Coefficients in (Fe$_{90}$Co$_{10}$)$_{78}$Si$_{12}$B$_{10}$-AlN Thin Film Composites. *Appl. Phys. Lett.* **2010**, *96*, 182501.
3. Manfred, F. Revival of the Magnetoelectric Effect. *J. Phys. D: Appl. Phys.* **2005**, *38*, R123.
4. Pedro, M.; Senentxu, L. M. Polymer-Based Magnetoelectric Materials. *Adv. Funct. Mater.* **2013**, *23*, 3371–3385.
5. Choi, T.; Horibe, Y.; Yi, H. T.; Choi, Y. J.; Wu, W.; Cheong, S. W. Insulating Interlocked Ferroelectric and Structural Antiphase Domain Walls in Multiferroic YMnO$_3$. *Nat. Mater.* **2010**, *9*, 253–258.
6. Cheong, S. W.; Mostovoy, M. Multiferroics: A Magnetic Twist for Ferroelectricity. *Nat. Mater.* **2007**, *6*, 13–20.
7. Kimura, T.; Goto, T.; Shintani, H.; Ishizaka, K.; Arima, T.; Tokura, Y. Magnetic Control of Ferroelectric Polarization. *Nature* **2003**, *426*, 55–58.
8. Wang, J.; Neaton, J. B.; Zheng, H.; Nagarajan, V.; Ogale, S. B.; Liu, B.; Viehland, D.; Vaithyanathan, V.; Schlom, D. G.; Waghmare, U. V.; *et al.* Epitaxial BiFeO$_3$ Multiferroic Thin Film Heterostructures. *Science* **2003**, *299*, 1719–1722.
9. Choi, T.; Lee, S.; Choi, Y. J.; Kiryukhin, V.; Cheong, S. W. Switchable Ferroelectric Diode and Photovoltaic Effect in BiFeO$_3$. *Science* **2009**, *324*, 63–66.
10. Chu, Y. H.; Martin, L. W.; Holcomb, M. B.; Gajek, M.; Han, S. J.; He, Q.; Balke, N.; Yang, C. H.; Lee, D.; Hu, W.; *et al.* Electric-Field Control of Local Ferromagnetism Using a Magnetoelectric Multiferroic. *Nat. Mater.* **2008**, *7*, 478–482.
11. Horiuchi, S.; Tokunaga, Y.; Giovannetti, G.; Picozzi, S.; Itoh, H.; Shimano, R.; Kumai, R.; Tokura, Y. Above-Room-Temperature Ferroelectricity in a Single-Component Molecular Crystal. *Nature* **2010**, *463*, 789–792.
12. Baker, W. J.; Ambal, K.; Waters, D. P.; Baarda, R.; Morishita, H.; Schooten, K.; Mccamey, D. R.; Lupton, J. M.; Boehme, C. Robust Absolute Magnetometry with Organic Thin-Film Devices. *Nat. Commun.* **2012**, *3*, 898.
13. Zang, H.; Yan, L.; Li, M.; He, L.; Gai, Z.; Ivanov, I.; Wang, M.; Chiang, L.; Urbas, A.; Hu, B. Magneto-Dielectric Effects Induced by Optically-Generated Intermolecular Charge-Transfer States in Organic Semiconducting Materials. *Sci. Rep.* **2013**, *3*, 2812.
14. Ren, S.; Wuttig, M. Organic Exciton Multiferroics. *Adv. Mater.* **2012**, *24*, 724–727.
15. Jin, J.; Lu, S. G.; Chanthad, C.; Zhang, Q.; Haque, M. A.; Wang, Q. Multiferroic Polymer Composites with Greatly Enhanced Magnetoelectric Effect under a Low Magnetic Bias. *Adv. Mater.* **2011**, *23*, 3853–3858.
16. Lunkenheimer, P.; Müller, J.; Krohns, S.; Schrettle, F.; Loidl, A.; Hartmann, B.; Rommel, R.; de Souza, M.; Hotta, C.; Schlueter, J. A.; *et al.* Multiferroicity in an Organic Charge-Transfer Salt That Is Suggestive of Electric-Dipole-Driven Magnetism. *Nat. Mater.* **2012**, *11*, 755–758.
17. Tayi, A. S.; Shveyd, A. K.; Sue, A. C. H.; Szarko, J. M.; Rolczynski, B. S.; Cao, D.; Kennedy, T. J.; Sarjeant, A. A.; Stern, C. L.; Paxton, W. F.; *et al.* Room-Temperature Ferroelectricity in Supramolecular Networks of Charge-Transfer Complexes. *Nature* **2012**, *488*, 485–489.
18. Wu, M.; Burton, J. D.; Tsymbal, E. Y.; Zeng, X. C.; Jena, P. Multiferroic Materials Based on Organic Transition-Metal Molecular Nanowires. *J. Am. Chem. Soc.* **2012**, *134*, 14423–14429.
19. Thomas, S.; Ramasesha, S.; Hallberg, K.; Garcia, D. Fused Azulenes as Possible Organic Multiferroics. *Phys. Rev. B* **2012**, *86*, 180403.
20. Wu, M.; Burton, J. D.; Tsymbal, E. Y.; Zeng, X. C.; Jena, P. Hydroxyl-Decorated Graphene Systems as Candidates for Organic Metal-Free Ferroelectrics, Multiferroics, and High-Performance Proton Battery Cathode Materials. *Phys. Rev. B* **2013**, *87*, 081406.

21. Stroppa, A.; Barone, P.; Jain, P.; Perez, J. M.; Picozzi, S. Hybrid Improper Ferroelectricity in a Multiferroic and Magnetoelectric Metal-Organic Framework. *Adv. Mater.* **2013**, *25*, 2284–2290.

22. Hu, B.; Yan, L.; Shao, M. Magnetic-Field Effects in Organic Semiconducting Materials and Devices. *Adv. Mater.* **2009**, *21*, 1500–1516.

23. Hu, B.; Wu, Y. Tuning Magnetoresistance between Positive and Negative Values in Organic Semiconductors. *Nat. Mater.* **2007**, *6*, 985–991.

24. Nguyen, T. D.; Ehrenfreund, E.; Vardeny, Z. V. Spin-Polarized Light-Emitting Diode Based on an Organic Bipolar Spin Valve. *Science* **2012**, *337*, 204–209.

25. Dang, M. T.; Hirsch, L.; Wantz, G. P3HT:PCBM, Best Seller in Polymer Photovoltaic Research. *Adv. Mater.* **2011**, *23*, 3597–3602.

26. Clarke, T. M.; Ballantyne, A. M.; Nelson, J.; Bradley, D. D. C.; Durrant, J. R. Free Energy Control of Charge Photogeneration in Polythiophene/Fullerene Solar Cells: The Influence of Thermal Annealing on P3HT/PCBM Blends. *Adv. Funct. Mater.* **2008**, *18*, 4029–4035.

27. Bussac, M. N.; Zuppiroli, L. Bipolaron Singlet and Triplet States in Disordered Conducting Polymers. *Phys. Rev. B* **1993**, *47*, 5493–5496.

28. Kahol, P. K.; Spencer, W. R.; Pinto, N. J.; McCormick, B. J. Magnetic-Susceptibility Analysis of Polyaniline and Its Derivatives in Terms of Triplet Bipolarons. *Phys. Rev. B* **1994**, *50*, 18647–18650.

29. Qin, W.; Yin, S.; Gao, K.; Xie, S. J. Investigation on Organic Magnetoconductance Based on Polaron−Bipolaron Transition. *Appl. Phys. Lett.* **2012**, *100*, 233304.

30. Silva, C. Organic Semiconductors: A Little Energy Goes a Long Way. *Nat. Mater.* **2010**, *9*, 884–885.

31. Baldo, M. A.; O'Brien, D. F.; You, Y.; Shoustikov, A.; Sibley, S.; Thompson, M. E.; Forrest, S. R. Highly Efficient Phosphorescent Emission from Organic Electroluminescent Devices. *Nature* **1998**, *395*, 151–154.

32. Qin, W.; Gao, K.; Yin, S.; Xie, S. J. Investigating the Magnetic Field Effect on Electron−Hole Pair in Organic Semiconductor Devices. *J. Appl. Phys.* **2013**, *113*, 193901.

33. Köhler, A.; Beljonne, D. The Singlet−Triplet Exchange Energy in Conjugated Polymers. *Adv. Funct. Mater.* **2004**, *14*, 11–18.

34. Blinc, R.; Žekš, B. Dynamics of Order-Disorder-Type Ferroelectrics and Anti-Ferroelectrics. *Adv. Phys.* **1972**, *21*, 693–757.